DOI: https://doi.org/10.53350/pjmhs22167716

ORIGINAL ARTICLE

Enhanced Photocatalytic Degradationof Rhodamine-BDye using Photocatalyst ZNO Sensitized by Visible Light

SHADIA FARHAN ABD[1], HASSAN ABBAS ALSHAMSI[2]
[1,2]Department of Chemistry, College of Education, University of Al-Qadisiyah, Diwaniya, Iraq
Corresponding author: Shadia Farhan Abd, Email: Sha1980f@gmail.com, Cell: +9647809687514

ABSTRACT

In the current study, zinc oxide nanoparticles in different concentrations were synthesized by environmentally friendly biosynthesis method using Argyreia nervosa leaf extract and used to remove Rhodamine-B dye. The structure, optical activity, morphology and porosity of the obtained nanomaterials were determined using different techniques including These include X-ray diffraction (XRD), field emission scanning electron microscopy (FE-SEM), elemental spectroscopy (EDX), and scanning electron microscopy (TEM), and fluorescence imaging. ultraviolet. The reflection spectroscopy (DRS) and Brunauer-Emmett-Teller (BET), and the zinc oxide chemical bond formations were confirmed by FT-IR, then the XRD results showed that the zinc oxide nanoparticles were successfully synthesized. TEM images of (ZnO-NPs) showed that the majority of the particles were spherical and weakly agglomerated, the best RhB stain removal was approached under ideal conditions (RhB = 5 ppm,10ppm,15ppm, pH = 11, catalyst dose = 1.4 g/L and time irradiation = 180 minutes). The high efficiency of the catalyst showed enhanced photocatalytic behavior for the degradation of RhB dye with a removal rate (48%) at 5ppm concentration, at a concentration of 10ppm about 31% and at concentration 15ppm the decomposition efficiency is 19%, without using any metal doping

Keywords: green synthesis, ZnO, Photodegradation, RhodamineB, Argyreia nervosa, mechanism.

INTRODUCTION

Pollution of natural water resources is a serious global issue [1]. Water is the primary source of life on Earth[2]. Organic materials, medicines, various products, biocides, heavy metals, dyes, and plastics are among the most important pollutants [3]. The wide spread of organic dyes in industrial wastewater from industries leads to significant environmental pollution [4]. Dyes can be classified into natural and synthetic pigments [5,6]. Synthetic dyes are widely used in coloring and printing activities such as the paper, textile, leather, and cosmetic industries, [7]. Rhodamine dye photocatalysis is a process that involves the photolysis of organic dirt on surfaces by applying visible light, ultraviolet light, or both to make these surfaces hydrophilicThe photolysis process begins when the surface of the semiconductor is irradiated [8]. Effect of the structural structure and pH of the solution on the photocatalytic efficiency [9]. Photocatalysis, an advanced oxidation process, has shown great potential for being cost-effective, environmentally friendly, solar water treatment and complete decomposition of organic pollutants [10]. There are two methods that can be applied to obtain ultra-high fluid resistance surfaces that are developing rough surfaces and treating rough surfaces with materials with low surface energy. [11] Zinc oxide (ZnO) nanoparticles attract a lot of attention due to theirwidespread use and nanotechnological properties [12] Reports have indicated both risks and benefits associated with the use of zinc oxide nanoparticles in a concentration-dependent manner and the method of synthesis[13] . Zinc oxide is characterized by a low cost, a band gap of about 3.37 eV, and a high binding energy of 60 mV [14-16]. It has advantages such as fixation on the substrate and especially the shape of zinc alloy with cubic lattice structure [17]. Among them, the metal oxides, ZnO exhibit ferroelectric, piezoelectric, catalytic, and photochemical properties [18]. Zinc oxide has many qualities, the main properties being semiconductivity, antimicrobial activity and UV absorption [19-24]. It is an important material frequently used in self-cleaning applications due to its high chemical and physical stability, oxidation capacity, and superior performance in decomposing organic molecules in basic and acidic aqueous solutions. [25,26]. Among the most important applications of zinc oxide are such as laser diodes, gas sensors, optoelectronic devices, and solar energy devices. ZnO nanostructures have been found to be used in nano-devices such as the nano gas sensor. ZnO in the form of nanostructures will enhance the properties of gas sensors due to its high surface area. Apart from this, the biologically safe properties of ZnO make it extremely important for biomedical applications. A method for economical mass production and determination of conditions so the synthesis of ZnO nanostructures will be very useful. That is why the study of the composition of ZnO nanostructures is of great technical importance [27] Nanotechnology is an emerging technology that can revolutionize various scientific fields. Nanomaterials have wide-ranging applications due to their size and conformation, and have been an important topic in the fields of basic and applied sciences. In recent years, there has been a great emphasis on nano-sized conductors due to their novel properties that have applications in optoelectronics. Among the many nanoparticles, zinc oxide nanoparticles (ZnONPs) are versatile semiconductors that exhibit significant optical transparency and luminescent properties in the ultraviolet-visible (UV-Vis) regions. These nanoparticles have become important in recent years, due to their excellent chemical and thermal stability. There are several to prepare nano-zinc oxide, such as sol-gel, hydrothermal, spray pyrolysis, microwave-assisted techniques, chemical vapor deposition, ultrasonic conditions and deposition methods [28-29].

To obtain nanoparticles in this paper, zinc oxide nanocomposites were synthesized using an environmentally friendly method and used to examine the photocatalytic activity of RhB dye removal from contaminated solutions. Nanomaterials have been described by XRD, FE-SEM, EDS, TEM, BET, DRS and FT-IR spectroscopy. The photocatalytic activity against RhB dye was studied under optimal conditions such as effect of catalyst dose, initial RhB dye concentration, irradiation time and pH effect. Study the effect of reactive oxygen scavengers. And to identify the most reactive species that contribute to the photolysis of RhB.

MATERIALS AND METHODS

Chemicals: All the chemicals obtained in this work were of high purity and were directly used without additional purification. ($Zn(NO_3)_2$. $6H_2O$99%), sodium hydroxide (NaOH 99.5%) and (Rhodamine- B 99.5%) 99% were purchased. From Sigma-Aldrich Chemie GmbH (Taufkirchen, Germany) was used, as well as solvents such as absolute ethanol 99.9%. and double-distilled water deionized during the experiments. Argyreia nervosa leaves have been used.

Characterization: The structural phases of the synthesized nanomaterial powders were studied using XRD measurements using nickel-filtered Cu Kα radiation (λ = 1.54056 nm) in the range 10°–80° (Shimadzu-Japan XRD 6000). It was identified using field emission scanning electron microscopy (FE-SEM) using JSM-6701 (JEOL, Japan) and transmission electron microscopy (TEM) analysis using FEI Tecnai TF20 is 200 kV. DRS-UV-Vis spectra were measured in the 200-800 nm range using a Shimadzu-Japanese UV-Vis 160V spectrophotometer. The specific surface

area and pore size were determined by Brunauer-Emmett-Teller (BET) analysis of N2 adsorption using QuadrasorbSIMP. A dual-UV spectrophotometer was used to read the UV visible absorption (UV-1650, Shimadzu).Fourier transform infrared spectroscopy (Bruker-FTIR) was conducted by using KBr pallet in the range of (4000–400 cm^{-1}).

Preparation of plant extract: For the purpose of preparing a plant extract with a concentration of 10%, we take the leaves of the Argyreia nervosaleaf plant and wash them with distilled water and dry them under the sun until they are completely dry. At 50 ° C for 30 minutes, then we filter the plant extract to obtain a clear substance free of suspended matter and put it in sealed bottles for the purpose of using it in the preparation of nanomaterials.

Synthesis of Nanocomposites ZnO:

A Sample-(1) preparation of zinc oxide at a concentration of (0.1M : Zinc oxide is prepared in an environmentally friendly manner by using the extract of the leaves of the creeping elephant plant at a concentration of 10% of the plant extract. We put in a 250 ml beaker 50 ml distilled water and add to it 1.48 g of aqueous zinc nitrate $Zn(NO_3)_2.6H_2O$ and heated to 50 degrees 30 minutes and add the plant extract for two hours. From light yellow to faint yellow, where the nucleation process begins, where the PH becomes about 12, and heating continues for two hours at a temperature of 50 degrees Celsius, then it is left for 24 hours to form the precipitate, and then the washing and separation phase of the precipitate begins, where the washing is done with ethanol concentration of 99% to purify it from and after it is used Centrifuge 8000, then distilled alcohol, then distilled water, and the process of washing and separating the precipitate continues to pH = 7 and then drying the Rasperin machine. At a temperature of 80 ° C, suitable for 4 hours, then transferred to the nano-burning furnace (ZnO NPs) [30-31].

B The Sample (2) preparation of zinc oxide with a concentration of (0.2M) : We put in a beaker a capacity of 250 ml 50 ml of distilled water and add to it 2.97 g of aqueous zinc nitrate $Zn(NO_3)_2.6H_2O$ and heat at 50 ° C with continuous stirring for 10 minutes and add to it the plant extract at a concentration of 10% with Heating for two hours During this period we add sodium hydroxide NaOH at a concentration of 1 M (2 g of sodium hydroxide dissolve in 50 ml of distilled water) add to the mixture drop by drop until the color changes from light yellow to faint yellow where the nucleation process begins until the pH becomes about 12 and continues Heating for another two hours at a temperature of 50 degrees Celsius, then leaving the solution for 24 hours to form the precipitate, then the washing and separation stage of the precipitate, where washing is done with ethanol, which has a concentration of 99% to purify it from impurities and is separated by a centrifuge at 8000 cycles per minute for 10 minutes and then washed with distilled water, then With alcohol and then distilled water, the washing and separation process is repeated until we get pH = 7, and then the process of drying the precipitate is done in a hot air oven at 80 degrees Celsius for a period of 4 hours, then it is transferred to the burning oven for the purpose of calcination and for a period of 4 hours at a temperature of 500 degrees Celsius, and then make sure that the zinc nitrate is reduced to zinc ions by changing the color from yellow to white, and the white solid substance formed is zinc nanoparticles ZnO Nps [32-33].

Photodegradation oF Rhodamine B dye: To study the photocatalytic activity of photocatalysts, the RhB dye was used as a staining model. A Xenon 100 w lamp was used as a visible light source for dye processing. In this regard, a known amount of the photocatalyst was suspended in 100 ml of aqueous dye solution with magnetic stirring for 90 min in the dark at 60 °C to ensure that the adsorption-desorption equilibrium occurred. Then, the mixture was exposed to visible light irradiation with continuous magnetic stirring for 180 min. After a certain time, 2 ml of the radioactive solution was withdrawn, and separated at 8000 rpm for 15 min to remove the photocatalyst nanoparticles and obtain a clear supernatant. Then, the absorbance of the residual RhB dye was measured using a UV visible spectrophotometer at the dye's maximum wavelength (λmax = 554 nm). The effect of various factors including irradiation time (0-180 min), catalyst dose (1 g/L), pH = 11 and initial RhB concentration efficiency (5ppm) on photolysis efficiency was investigated. The photolysis efficiency (PDE%) of the dye was calculated using the following equation:

Photodegradation efficient (PDE%) = $[(C_o - C_t) / C_o] \times 100$……..(1)

Where, C_o is the initial concentration of RhB dye, Ct is the concentration of RhB dye at time (t) [34].

Determine the lambdamax of Rh-B dye: In order to determine the maximum wavelength of Rh-B dye, the UV and visible absorption spectra of the dye solution were recorded at concentration (10ppm) and the wavelength was fixed by a UV spectrophotometer. Within the range from (200-800 nm), where the maximum wavelength of Rh-B dye solution was determined at its highest absorbance in the UV and visible spectrum, where the greatest wavelength of Rh-B dye was λmax=553nm.

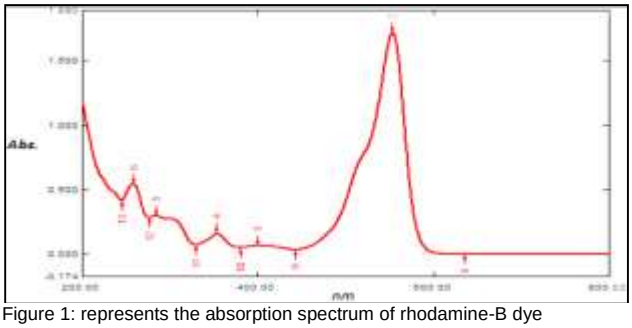

Figure 1: represents the absorption spectrum of rhodamine-B dye

Titration curve for rhodamine - B dye: The titration value of rhodamine dye Rh-B was drawn by preparing a group of dye solutions with different concentrations of (5-15ppm). At wavelength(λ_{max} =553nm) the focus that is in the Beer-Lambert Law area of application.

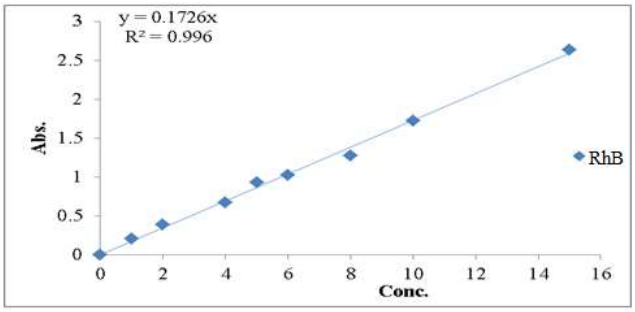

Figure 2: titration curve of rhodamine-B dye

RESULTS AND DISCUSSION

X-ray diffraction (XRD): To determine the crystalline shape and size of the synthesized nanomaterials were analyzed by X-ray technique. Figure 1 shows the XRD diffraction of zinc oxide,The diffraction peaks are observed to appear at (2θ = 31.86◦, 34.53◦, 36.41◦, 46.17◦, 56.76◦, 62.91◦, 63.05◦, 66.40◦ ,68.02◦, 69.20◦, 72.84◦, 77.01◦) assigned to Miller levels (100), (002), (101) (210) , (011), (103), (220), (002), (112), (120), (202), respectively of ZnO crystals in cubic shape and hexa wurtzite and this agrees with the (JCPDS card No. 036-1451). these prominent and clear peaks indicate the formation of the pure zinc oxide compound that appeared in the previous results [35].

Scanning Electron Microscope (FE-SEM) analysis: Surface characteristics of the morphology of zinc oxide nanoparticles with different proportions in terms of particle size, shape and agglomeration, as well as the distribution of these particles. The

properties and effectiveness of zinc dioxide, depend to a large extent on the nature and shape of their surface. show scanning electron microscope images of nanoparticles (ZnO) as shown in Fig. (a) is an image of oxide particles zinc nanoparticles. The results of the examination showed that the zinc oxide particles have a spherical shape with an average fine size between (30-90 - nm) in addition. The particles tend to agglomerate less as a result of the ultrasonic effect which disperses these small particles and prevents them from agglomerating or accumulating too much, and the presence of some agglomerations is due to polar attraction and weak electrostatic forces (Wanderwales) in addition to the calcination process which has an effect that is very difficult to avoid due to the use of high temperatures (500 °C) to complete the growth process ZnO crystals [36].

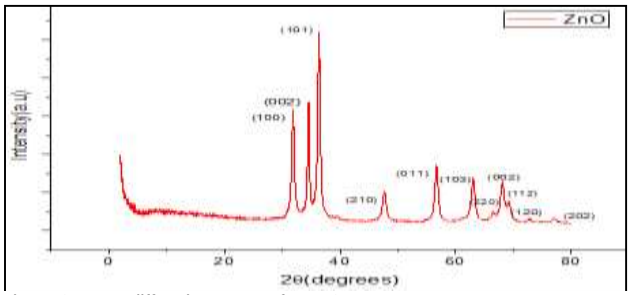

Figure 3: X-ray diffraction pattern for ZnO

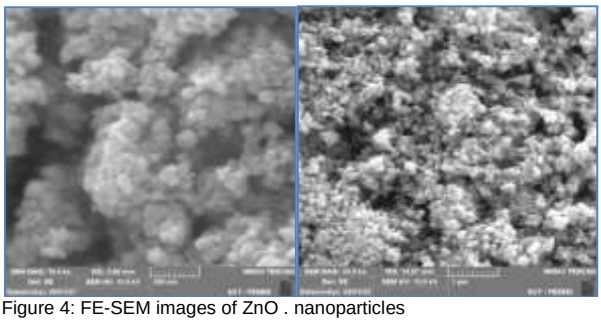
Figure 4: FE-SEM images of ZnO . nanoparticles

Dispersive X-ray Spectroscopy (EDX) Energy: The EDX spectrum is used to analyze the proportion of the elements present in the prepared oxides and nanocomposites. The results of the EDX analysis proved the presence of ZnO NPs. The results also confirmed the atomic ratios as shown in Table .1 for zinc and oxygen, and this evidence confirms the formation of nano-zinc oxide.

Table 1: shows the values of oxygen and zinc in ZnO

Element	Weight%	Atomic%	Summation
Zn	79.4	43.41	100%
O	20.6	56.59	

Transmission electron microscopy (TEM) analysis: The TEM images showed that the majority of the particles were spherical aggregated, where homogeneous ZnO nanoparticles with spherical shapes and weak agglomeration were observed as shown in Figure (a). [37]. Ultrasound is responsible for the scaling and contraction of nanoparticles, and. The average nanoparticle size was calculated from measurements of more than (150) nanoparticles in the random fields of the TEM grid. The size of the zinc oxide nanoparticles ranged around (20.37 nm) and this indicates the success and accuracy of the method of preparing the zinc oxide nanocomposite [38].

Surface area analysis (BET,BJH): Depending on the adsorption-desorption isotherms, the surface area of the prepared samples was determined by the Brunauer-Emmett-Teller (BET)way and the results are shown in Figure (5a) the nitrogen adsorption-desorption BET isotherm on the surface of the zinc oxide compound and Table (2) Surface Area Analysis (BET, BJH)also also shows the pore size distribution according to the BJH isotherm if the surface area of ZnO is about (11.83 m^2g^{-1}) and the pore diameter range is (55.2nm) and the size The porosity is (4.20 cm3 g-1), and the figure(5. b) shows the nitrogen adsorption-desorption isotherm on the surface of iron oxide according to the BET isotherm (11.088cm^3 g^{-1}) The pore diameter range is (14,572 nm) according to the BJH isotherm [39] . this indicates that the prepared composites are of the Microporous type of solid porous materials that have a pore size ranging within the range (2-50 nm). According to the classification of the International Union of Pure and Applied Chemistry (IUPAC) [40] .

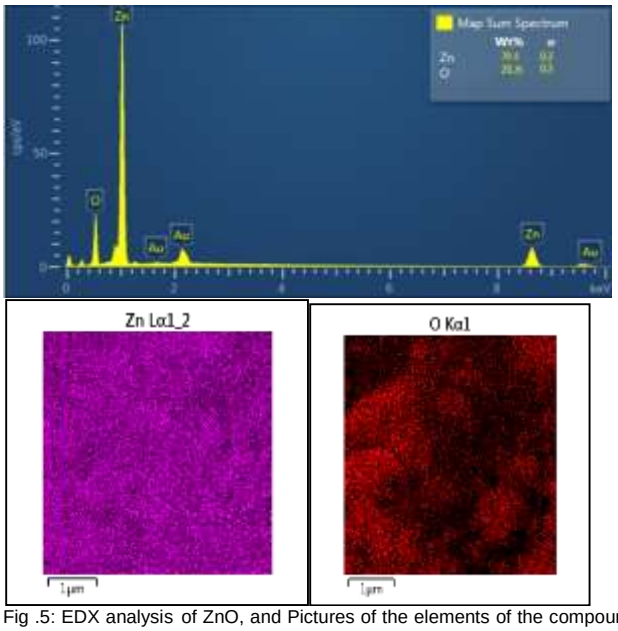

Fig .5: EDX analysis of ZnO, and Pictures of the elements of the compound ZnO

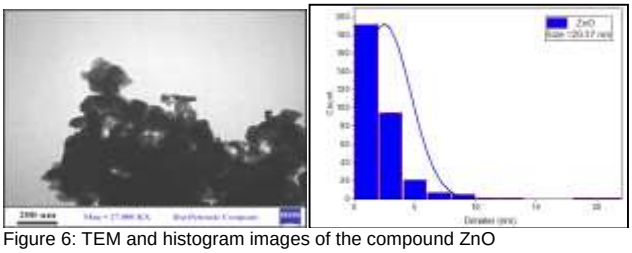
Figure 6: TEM and histogram images of the compound ZnO

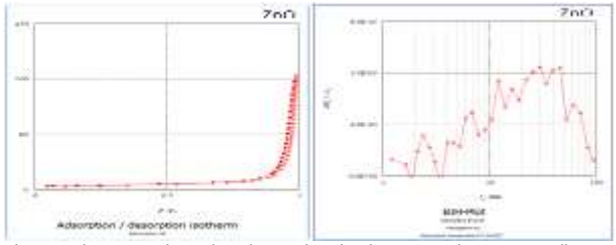

Fig. 7: Nitrogen adsorption-desorption isotherms and corresponding pore size distributioncurve ofZnO

Ultraviolet Reflection-Scattering Spectrum (DRS): The optical properties of ZnO nanostructures were studied using ultraviolet diffused reflection spectroscopy (UV-Vis DRS), as shown in Figure (a). Unpaired ZnO showed strong adsorption in the UV region with a distinct absorption edge at nm378 which can be assigned to the

intrinsic bandgap absorption of ZnO due to electron transitions from the valence band to the conduction band (O2p → Zn3d). [41] The absorption edge of ZnO corresponds to Previously reported absorption peaks for ZnO are within the spectral range 350-390 nm [42-43]. In semiconductors, the energy bandgap can be determined (for example) using the relationship between the absorption coefficient (α) and the energy of the incident photon (hv) near the edge of the optical range as shown in Tauc's equation:

$(\alpha\ h\nu)^2 = A(h\nu - Eg)$……(2)

α / represents the absorption coefficient, V/ the frequency of light, h / Planck's constant, A/ the proportionality constant .

As figure .6b show, extrapolation of the linear region of $(\alpha h\nu)^2$ vs. hv plots provides the bandgap (E_g) for the synthesized nanoparticles. The spectral absorption edge of ZnO corresponds to a band gap of 3.2 eV.

Table 2: Surface Area Analysis (BET, BJH)

Sample	Surfac earea (m^2/g)	Pore volume (cm^3/g)	Pore Diamete r(nm)	Type of pore	Hysteresis (p/po)
ZnO	1.8305	4.2056	55.266	Microporous	H3

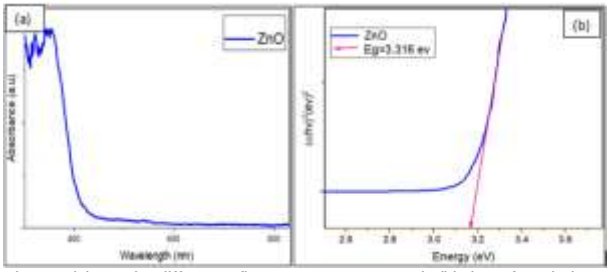

Fig .6: (a)UV-vis diffuse reflectance spectra and (b)plot of variation of ($ahv)^2(ev)^2$ photon energy for ZnO

Fourier transform infrared Spectroscopy (FT-IR): The infrared spectrum is widely used in diagnosing the prepared nanocomposites, if it gives an idea of the type of interference between the components of the nanocomposite.(4000-400 cm^{-1}) and the IR spectrum of the compound zinc oxide (ZnO) showed the presence of a broad band at 3434 cm^{-1} and a weak band at frequency 1500 cm^{-1} due to the stretching vibrations of the carboxyl group (O-H) and due to the water molecules adsorbed on the surface of the zinc oxide In addition to the presence of another residing band at the frequency region between 416 $cm^{-1,}$ which belongs to zinc oxide (Zn-O), and this diagnostic band confirms that it is zinc oxide [44]. 2879 cm^{-1} belongs to carbonated species to CO2 from the atmosphere [45].

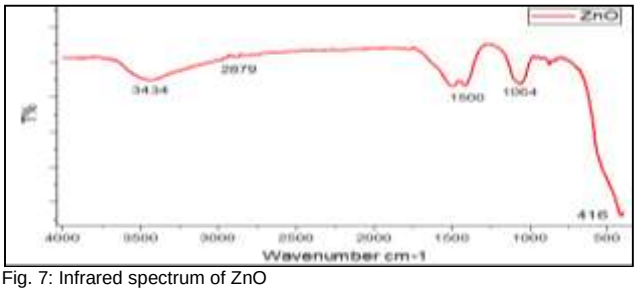

Fig. 7: Infrared spectrum of ZnO

Study of the Photocatalyst activity of the catalyst: In order to study the catalytic activity of zinc oxide and its efficiency in cracking Rhodamine B dye, Rhodamine B dye was prepared with RhB concentration = 5 ppm, Catalyst dose = 1.0 g/L, pH 11, T = 298 K, irradiation time = 180 min) . Zinc oxide was tested under the same conditions as a function of illumination time. appearance. It was found that treating the dye with zinc oxide as a photocatalyst shows a decomposition efficiency at 5ppm concentration about 48%, at a concentration of 10ppm about 31% and at concentration 15ppm the decomposition efficiency is 19%, therefore zinc oxide and visible light alone cannot decompose the dye. The results clearly indicate that the bandgap is lower than the conduction band of ZnO, which is mainly responsible for visible light absorption and thus narrows the bandgap of ZnO. Zinc oxide must be impregnated with metal oxides.

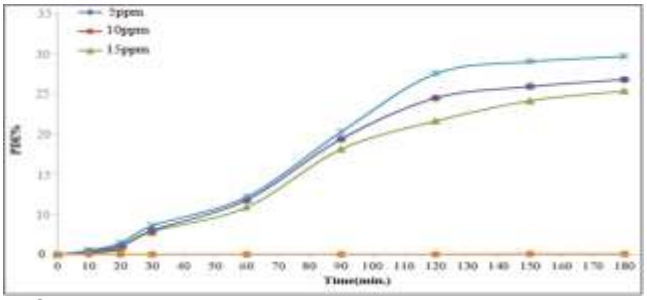

Fig.**8**: Demonstrates the catalytic activity of zinc oxide ZnO

Photo-Degradation Mechanism ZnO: ZnO is an n-type semiconductor with a direct and wide band gap in the near-UV spectral region (≥3.32 eV) and high electron mobility [46]. The ZnO electronic structure provides photocatalytic activity, giving ZnO unique multifunctional properties. When ZnO is excited by a radiation of energy equal to or greater than the band gap (Eg), excited electrons move to the conduction band (e^-_{CB}), leaving behind holes in the valence band (h^+_{VB}) [47].

$ZnO + hu \rightarrow ZnO\ (h^+_{VB} + e^-_{CB})$……(1)

$h^+_{VB} + H_2O \rightarrow OH + H^+$ ……..(2)

$e^-_{CB} + O_2 \rightarrow {}^{\cdot}O_2^-$……..(3)

${}^{\cdot}O_2^- + H^+ \rightarrow HO_2^{\cdot}$ .....(4)

$HO_2^{\cdot} + HO_2^{\cdot} \rightarrow H_2O_2 + O_2$……..(5)

$e^-_{CB} + H_2O_2 \rightarrow {}^{\cdot}OH + OH^-$…….... (6)

${}^{\cdot}OH + RhB \rightarrow$ Degradation products$\rightarrow CO_2 + H_2O$……(7)

This process is schematically presented in Figure.8. ZnO is

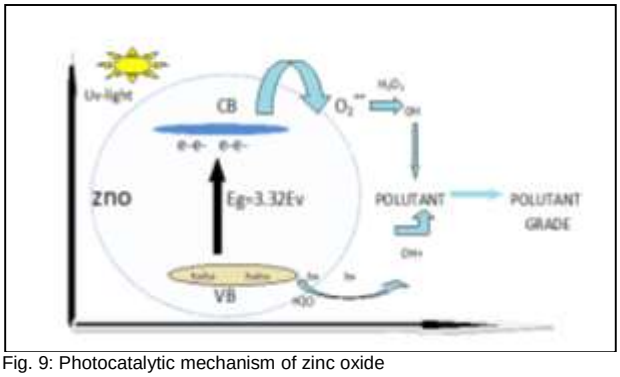

Fig. 9: Photocatalytic mechanism of zinc oxide

CONCLUSION

The present study reported that the present work is economically viable, environmentally friendly, effective and safe for green preparation of ZnO NPs using Argyreia nervosa leaf extract without using any toxic or hazardous substance. The as-prepared nanomaterials possess a crystal system with more than one crystal form, the results showed that the illumination of the dye solution catalyst showed negligible photodegradation efficiency, thus light alone cannot degrade the dye molecules. As the results showed,

so the zinc oxide must be doped with transition elements for the purpose of narrowing the energy gap. This was because the surface of the zinc oxide is included with an appropriate amount of metal oxides that enhances the absorption of visible light. remarkably, The time-dependent photo-catalytic activities of pure and doped samples of ZnO were studied separately under irradiation of UV–visible and visible light by degradation of Rhodamine B dye. The high efficiency of the catalyst showed enhanced photocatalytic behavior for the degradation of RhB dye with a removal rate (48%) at 5ppm concentration, at a concentration of 10ppm about 31% and at concentration 15ppm the decomposition efficiency is 19%, without using any metal doping.

REFRENCES

1 B OGNÁR, Szabolcs; PUTNIK, Predrag; ŠOJIĆ MERKULOV, Daniela. Sustainable green nanotechnologies for innovative purifications of water: Synthesis of the nanoparticles from renewable sources. Nanomaterials, 2022, 12.2: 263.

2 ZAMORA-LEDEZMA, Camilo, et al. Heavy metal water pollution: A fresh look about hazards, novel and conventional remediation methods. Environmental Technology & Innovation, 2021, 22: 101504.

3 KALBAR, Pradip P. Hybrid treatment systems: a paradigm shift to achieve sustainable wastewater treatment and recycling in India. Clean Technologies and Environmental Policy, 2021, 23.4: 1365-1373.

4 Y.-H. Chiu, T.-F.M. Chang, C.-Y. Chen, M. Sone, Y.-J. Hsu, Catalysts 9 (5) (2019) 430

5 PAVITHRA, K. Grace, et al. Removal of colorants from wastewater: A review on sources and treatment strategies. Journal of Industrial and Engineering Chemistry, 2019, 75: 1-19.

6 LAI, Xiaoxu, et al. Rapid microwave-assisted bio-synthesized silver/Dandelion catalyst with superior catalytic performance for dyes degradation. Journal of hazardous materials, 2019, 371: 506-512.

7 SHABANI, Maryam, et al. Mesoporous-mixed-phase of hierarchical bismuth oxychlorides nanophotocatalyst with enhanced photocatalytic application in treatment of antibiotic effluents. Journal of Cleaner Production, 2019, 207: 444-457.

8 LAI, Xiaoxu, et al. Rapid microwave-assisted bio-synthesized silver/Dandelion catalyst with superior catalytic performance for dyes degradation. Journal of hazardous materials, 2019, 371: 506-512.

9 RAFIQ, Asma, et al. Photocatalytic degradation of dyes using semiconductor photocatalysts to clean industrial water pollution. Journal of Industrial and Engineering Chemistry, 2021, 97: 111-128.

10 Q. Jing, et al., ACS Appl. Nano Mater. 1 (6) (2018) 2653

11 K. Khanmohammadi Chenab, B. Sohrabi, and A. Rahmanzadeh,Superhydrophobicity: advanced biological and biomedical applications, Biomater. Sci., 7(2019), No. 8, p. 3110.

12 GUR, Tuğba, et al. Green synthesis, characterization and bioactivity of biogenic zinc oxide nanoparticles. Environmental Research, 2022, 204: 111897.

13 CZYŻOWSKA, Agnieszka; BARBASZ, Anna. A review: zinc oxide nanoparticles–friends or enemies?. International Journal of Environmental Health Research, 2022, 32.4: 885-901.

14 ABEBE, Buzuayehu; MURTHY, HC Ananda; AMARE, Enyew. Enhancing the photocatalytic efficiency of ZnO: Defects, heterojunction, and optimization. Environmental nanotechnology, monitoring & management, 2020, 14: 100336.

15 MOIZ, Muhammad Abdul, et al. Enhancement of dye degradation by zinc oxide via transition-metal doping: a review. Journal of Electronic Materials, 2021, 50.9: 5106-5121.

16 ABDELSAMAD, Ahmed MA, et al. Enhanced photocatalytic degradation of textile wastewater using Ag/ZnO thin films. Journal of Water Process Engineering, 2018, 25: 88-95.

17 SANG, Nguyen Xuan, et al. Mechanism of enhanced photocatalytic activity of Cr-doped ZnO nanoparticles revealed by photoluminescence emission and electron spin resonance. Semiconductor Science and Technology, 2019, 34.2: 025013.

18 PARIHAR, Vandana; RAJA, Mohan; PAULOSE, Rini. A brief r eview of structural, electrical and electrochemical properties of zinc oxide nanoparticles. Reviews on Advanced Materials Science, 2018, 53.2: 119-130.

19 AHMOUM, H., et al. Impact of position and concentration of sodium on the photovoltaic properties of zinc oxide solar cells. Physica B: Condensed Matter, 2019, 560: 28-36.

20 GRASLAND, François, et al. About thermo-oxidative ageing at moderate temperature of conventionally vulcanized natural rubber. Polymer Degradation and Stability, 2019, 161: 74-84.

21 XIE, Zheng-Tian, et al. Effects of graphene oxide on the strain-induced crystallization and mechanical properties of natural rubber crosslinked by different vulcanization systems. Polymer, 2018, 151: 279-286

22 ZAKI, Nur Athirah Ahmad; MAHMUD, Shahrom; OMAR, Ahmad Fairuz. Ultraviolet protection properties of commercial sunscreens and sunscreens containing ZnO nanorods. In: Journal of Physics: Conference Series. IOP Publishing, 2018. p. 012012.

23 GRASLAND, François, et al. About thermo-oxidative ageing at moderate temperature of conventionally vulcanized natural rubber. Polymer Degradation and Stability, 2019, 161: 74-84.

24 XIE, Zheng-Tian, et al. Effects of graphene oxide on the strain-induced crystallization and mechanical properties of natural rubber crosslinked by different vulcanization systems. Polymer, 2018, 151: 279-286

25 ZAKI, Nur Athirah Ahmad; MAHMUD, Shahrom; OMAR, Ahmad Fairuz. Ultraviolet protection properties of commercial sunscreens and sunscreens containing ZnO nanorods. In: Journal of Physics: Conference Series. IOP Publishing, 2018. p. 012012.

26 ZHANG, Ranran, et al. Novel micro/nanostructured TiO2/ZnO coating with antibacterial capacity and cytocompatibility. Ceramics International, 2018, 44.8: 9711-9719.

27 ALAM, Syed Nasimul, et al. SEM, EDX & XRD of zinc oxide nanostructures synthesized by zinc oxidation. Microscopy and Analysis, 2012, 26.4: 11-14.

28 Omri, K.; Najeh, I.; Dhahri, R.; El Ghoul, J.; Elmir, L. Microelectron. Eng. 2014, 128, 53–58.

29 Zak, A.K.; Abrishami, M.E.; Majidi, W.H.; Abd Yosefi, R.; Hosseini, S.M. Ceram. Inter. 2011, 37, 393–398.

30 Wang, Y.; Zhang, C.; Bi, S.; Luo, G. Powder Technol. 2010, 202, 130–136.

31 YOONUS, Jumna; RESMI, R.; BEENA, B. Evaluation of antibacterial and anticancer activity of green synthesized iron oxide (α-Fe2O3) nanoparticles. Materials Today: Proceedings, 2021, 46: 2969-2974.

32 DEGEFA, Anatol, et al. Green synthesis, characterization of zinc oxide nanoparticles, and examination of properties for dye-sensitive solar cells using various vegetable extracts. Journal of Nanomaterials, 2021.

33 CHEMINGUI, H., et al. Facile green synthesis of zinc oxide nanoparticles (ZnO NPs): Antibacterial and photocatalytic activities. Materials Research Express, 2019, 6.10: 1050b4.

34 AO, Xiuwei; LIU, Wenjun. Degradation of sulfamethoxazole by medium pressure UV and oxidants: peroxymonosulfate, persulfate, and hydrogen peroxide. Chemical Engineering Journal, 2017, 313: 629-637.

35 FAKHARI, Shabnam; JAMZAD, Mina; KABIRI FARD, Hassan. Green synthesis of zinc oxide nanoparticles: a comparison. Green chemistry letters and reviews, 2019, 12.1: 19-24.

36 ALVER, Ü. M. İ. T., et al. Optical and dielectric properties of PMMA/α-Fe2O3–ZnO nanocomposite films. Journal of Inorganic and Organometallic Polymers and Materials, 2019, 29.5: 1514-1522.

37 VINAYAGAM, Ramesh, et al. Structural characterization of green synthesized α-Fe2O3 nanoparticles using the leaf extract of Spondias dulcis. Surfaces and Interfaces, 2020, 20: 100618.

38 ALVER, Ü. M. İ. T., et al. Optical and dielectric properties of PMMA/α-Fe2O3–ZnO nanocomposite films. Journal of Inorganic and Organometallic Polymers and Materials, 2019, 29.5: 1514-1522.

39 ELSHYPANY, Rania, et al. Elaboration of Fe3O4/ZnO nanocomposite with highly performance photocatalytic activity for degradation methylene blue under visible light irradiation. Environmental Technology & Innovation, 2021, 23: 101710.

40 NOUKELAG, S. K.; ARENDSE, C. J.; MAAZA, M. Biosynthesis of hematite phase α-Fe2O3 nanoparticles using an aqueous extract of Rosmarinus officinalis leaves. Materials Today: Proceedings, 2021, 43: 3679-3683.

41 PATIL, Santosh S., et al. Green approach for hierarchical nanostructured Ag-ZnO and their photocatalytic performance under sunlight. Catalysis Today, 2016, 260: 126-134.

42 LIAO, Peilin; CARTER, Emily A. Optical excitations in hematite (α-Fe2O3) via embedded cluster models: a CASPT2 study. The Journal of Physical Chemistry C, 2011, 115.42: 20795-20805.

43 AZIZI, Susan; MOHAMAD, Rosfarizan; MAHDAVI SHAHRI, Mahnaz. Green microwave-assisted combustion synthesis of zinc oxide nanoparticles with Citrullus colocynthis (L.) Schrad: characterization and biomedical applications. Molecules, 2017, 22.2: 301.

44 TOOBA, Simin; KIMIAGAR, Salimeh; ZARE-DEHNAVI, Nasser. The synthesis and characterization of α-Fe2O3 nanowires decorated with ZnO nanoparticles. International Journal of Modern Physics B, 2022, 36.06: 2250052.

45 CHAU, Jenny Hui Foong, et al. Advanced photocatalytic degradation of acetaminophen using Cu2O/WO3/TiO2 ternary composite under solar irradiation. Catalysis Communications, 2022, 163: 106396.

46 GHAYEMPOUR, Soraya; MONTAZER, Majid. Ultrasound irradiation based in-situ synthesis of star-like Tragacanth gum/zinc oxide nanoparticles on cotton fabric. Ultrasonics sonochemistry, 2017, 34: 458-465.

47 VERBIČ, Anja; GORJANC, Marija; SIMONČIČ, Barbara. Zinc oxide for functional textile coatings: Recent advances. Coatings, 2019, 9.9: 550.